A 24-GHz Ultra-Wideband Over Fiber System Using Photonic Generation and Frequency Up-Conversion

Qingjiang Chang, Yue Tian, Tong Ye, Junming Gao, and Yikai Su, *Senior Member, IEEE*

Abstract—**We propose and experimentally demonstrate the generation of baseband ultra-wideband (UWB) monocycle and doublet pulses using one dual-parallel Mach–Zehnder modulator. We further present a proof-of-concept demonstration of a 24-GHz UWB over fiber system based on frequency up-conversion. The performance of the up-converted UWB pulses after fiber transmission is studied.**

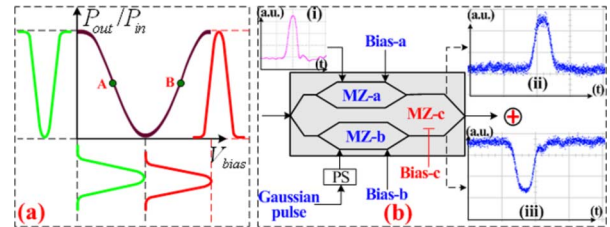*Index Terms*—**Dual-parallel Mach–Zehnder modulator (DPMZM), ultra-wideband (UWB) over fiber, up-conversion.**

Fig. 1. (a) Principle of monocycle pulse generation; (b) experimental demonstration of monocycle pulse generation. Waveform: 200 ps/div (t-axis).

I. INTRODUCTION

ULTRA-WIDEBAND (UWB) is a promising method to provide short-distance high-speed wireless communications in future 4G systems and wideband personal access networks [1]. There are two types of UWB signals: one is multiband orthogonal frequency-division multiplexing UWB, and the other is impulse-radio UWB (IR-UWB). IR-UWB is attractive due to the carrier-free advantage and better pass-through feature [2]. Recently, the convergence of UWB and optical fiber systems has raised great interest to extend the UWB coverage area and exploit the advantages offered by optical fibers. Monocycle and doublet pulses show good performances in IR-UWB systems. As it is complicated to directly produce them in the electrical domain, previous reports focused on optical generations of the baseband monocycle and doublet pulses using Gaussian driving signals [3]–[10]. Meanwhile, a 24-GHz UWB signal is desirable for its large bandwidth, spectrum availability, and high resolution. It has been defined as an emission mask fallen into the band of ∼22–29 GHz with a central frequency around 24 GHz and allocated for vehicular radar applications by the Federal Communications Committee (FCC) [11]. In addition, there is demand to integrate the local UWB environment into fixed wireline or wireless networks without distance limitation. Therefore, photonic frequency up-conversion is considered as one of the attractive techniques to generate the 24-GHz UWB signal [12], [13]. However, the performance of the up-converted UWB pulses after transmission has not been experimentally studied. Moreover, high-speed electrical devices are needed in [12] and an elaborated up-conversion structure is employed in [13].

The authors are with the State Key Laboratory of Advanced Optical Communication Systems and Networks, Department of Electronic Engineering, Shanghai Jiao Tong University, Shanghai 200240, China (e-mail: yikaisu@sjtu.edu.cn).

Color versions of one or more of the figures in this letter are available online at http://ieeexplore.ieee.org.

Digital Object Identifier 10.1109/LPT.2008.2002746

In this letter, we propose and demonstrate a 24-GHz UWB over fiber system with a simple structure using photonic generation and frequency up-conversion. An integrated dual-parallel Mach–Zehnder modulator (DPMZM) is used to optically generate UWB monocycle and doublet pulses. Since the DPMZM is a commercial off-the-shelf device fabricated on a single chip, compared to previous schemes employing multiple discrete components or complicated nonlinear processing [3]–[9], it exhibits the advantages of compact architecture, low cost, convenient alignment, and small insertion loss. The obtained baseband UWB is then up-converted to generate a 24-GHz UWB signal based on optical-carrier suppression (OCS) modulation. The performance of the up-converted UWB pulses after the fiber transmission is also studied.

II. UWB PULSE GENERATION

The DPMZM [14] consists of a pair of sub-Mach–Zehnder modulators (MZMs) embedded in the two arms of a main MZM. The two sub-MZMs have the same architecture and performance, and the main MZM combines the outputs of the two sub-MZMs. The output field of the main MZM can be given by

$$E_{\text{out\_MZ-c}}(t) = E_{\text{out\_MZ-a}} \exp\left(j\frac{\pi}{2} \cdot V_{\text{bias-c}}/V_{\pi\_c}\right)$$
$$+ E_{\text{out\_MZ-b}} \exp\left(-j\frac{\pi}{2} \cdot V_{\text{bias-c}}/V_{\pi\_c}\right) \quad (1)$$

where $E_{\text{out\_MZ-a}}$ and $E_{\text{out\_MZ-b}}$ are the output fields of the two sub-MZMs, $V_{\text{bias-c}}$ and V_{π_c} are the bias voltage and switching voltage of the main MZM, respectively. The output signals of the two sub-MZMs are constructively or destructively combined by adjusting the bias of the main MZM. Fig. 1(a) shows the generation principle of the UWB monocycle pulse based on the DPMZM. The MZMs have two modulation regions with opposite slopes at different bias voltages. If an electrical Gaussian pulse is applied to the two sub-MZMs biased at the positive (point A) and negative (point B) quadrature points, one can obtain optical pulses with inversed shapes, as depicted in Fig. 1(a). Fig. 1(b) shows an experimental
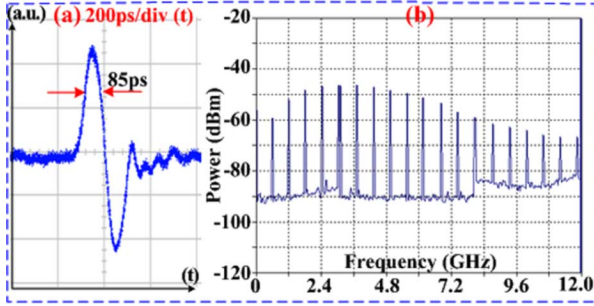
Fig. 2.   (a) Waveform of the generated monocycle pulse; (b) electrical spectrum of the generated monocycle pulse.
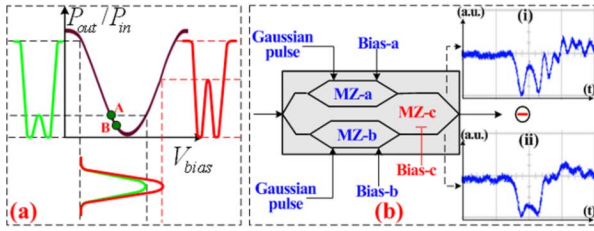

Fig. 3.   (a) Principle of doublet pulse generation; (b) experimental demonstration of doublet pulse generation. Waveform: 200 ps/div (t-axis).
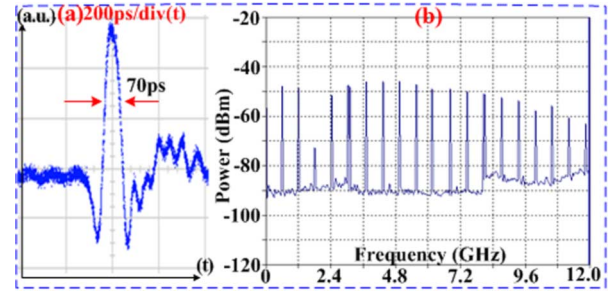

Fig. 4.   (a) Waveform of the generated doublet pulse; (b) electrical spectrum of the generated doublet pulse.
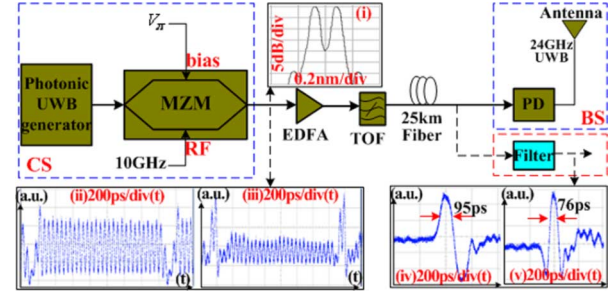

Fig. 5.   Experimental setup of the 24-GHz UWB over fiber system. (i) The spectrum of the OCS-UWB signal. (ii) and (iii) The waveforms of the OCS-UWB monocycle and doublet pulses, respectively. (iv) and (v) The waveforms of the filtered monocycle and doublet pulses, respectively.

illustration using a 10-GHz DPMZM (COVEGA Mach-10 060). A pulse pattern generator (PPG) is used to generate an electrical Gaussian pulse operating at 10 Gb/s with a fixed pattern of "1000 0000 0000 0000" [4], the waveform is shown in Fig. 1(b-i), where the full-width at half-maximum (FWHM) is ∼100 ps. The electrical Gaussian pulse is split into two equal parts to drive the two sub-MZMs, respectively. Two electrical amplifiers are required to amplify the electrical pulses. The output waveform from the MZ-a biased at the positive slope is shown in Fig. 1(b-ii) and the one from the MZ-b biased at the negative slope is provided in Fig. 1(b-iii). An electrical phase shifter (PS) is used to adjust the relative delay between the two modulating signals. In practice, the delay can also be realized by controlling the lengths of cables that connect the PPG and the two radio-frequency (RF) ports of the DPMZM, thus offering lower configuration cost. The outputs of the two sub-MZMs are constructively added by adjusting the bias-c to generate a monocycle pulse with an FWHM of ∼85 ps, as shown in Fig. 2(a). After detection by a photodetector (PD), the electrical spectrum is tested by an electrical spectrum analyzer in Fig. 2(b), where the central frequency is ∼4.5 GHz and the 10-dB bandwidth is ∼6 GHz (from 1.2 to 7.2 GHz). It should be noted that a polarity-reversed monocycle pulse can be obtained by adjusting the PS.

To obtain a doublet pulse, the nonlinear nature of the MZM transfer function can be utilized. If the MZM is biased such that the driving voltage crosses the transmission null of the MZM, certain overshoot can be generated, as indicated in Fig. 3(a). Fig. 3(b) shows the experimental demonstration using the same DPMZM. After being boosted by the electrical amplifiers, the two electrical Gaussian pulses with different amplitudes drive the MZ-a and the MZ-b, respectively, where the bias points are adjusted to be close to the transmission null (as shown in the point A and B of Fig. 3(a), respectively). The waveforms of the output signals from the MZ-a and the MZ-b are shown in insets (i) and (ii) of Fig. 3(b), respectively. The generated two

pulses are destructively combined so that a doublet pulse can be obtained. The waveform of the doublet pulse is shown in Fig. 4(a), where the FWHM is ∼70 ps. There are some ripples following the generated doublet pulse, which are attributed to the imperfect electrical driving pulses [see Fig. 1(b-i)]. The electrical spectrum is shown in Fig. 4(b), with the central frequency of ∼5 GHz and the 10-dB bandwidth of ∼7 GHz. A polarity-reversed doublet pulse can be obtained if the driving voltage crosses the transmission peak and bias points of the two sub-MZMs are set near the transmission maximum.

III. 24-GHz UWB Over Fiber Systems

Fig. 5 shows the experimental setup for the generation of the 24-GHz UWB over fiber system. The output optical field of the DPMZM can be given by

$$E_{\text{out\_DPMZM}} = \cos(\omega_o t) \cdot \cos[\alpha \cdot g(t)] \qquad (2)$$

where ω_o is the angular frequency of the optical carrier, α is modulation index, and $g(t)$ is the UWB pulse train. The optically modulated UWB signal from the DPMZM is injected into a following MZM, which is driven by an RF signal of the frequency ω_s, and biased at the transmission null to generate an OCS-UWB signal. Reference [15] has demonstrated a phase-modulated carrier is suppressed by the OCS technique. Using the Bessel functions, the output filed of the MZM can be approximately expressed as

$$E_{\text{MZM}} \approx E_o \cdot J_1(\beta) \cdot \{\cos[\alpha \cdot g(t)] \cdot \cos[(\omega_o - \omega_s)t] \\ + \cos[\alpha \cdot g(t)] \cdot \cos(\omega_o + \omega_s)t]\}. \qquad (3)$$
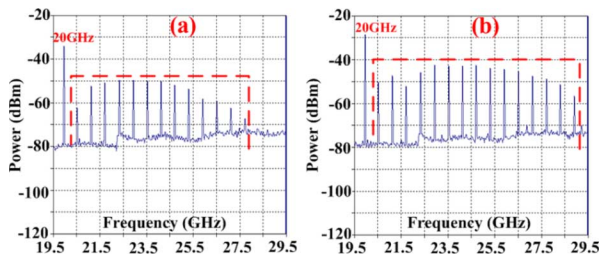
Fig. 6. Electrical spectra of the up-converted UWB pulses. (a) Monocycle pulse; (b) doublet pulse.

Fig. 7. (a) FWHM versus transmission distance; (b) BER curves.

Compared with (2), (3) shows that the UWB signal carried at the optical carrier is shifted to the two tones after the OCS modulation. In this experiment, the MZM is driven by a 10-GHz RF signal, thus generating a 20-GHz OCS-UWB signal; the spectrum is shown in Fig. 5(i). The optical eye diagrams of the up-converted UWB pulses are provided in Fig. 5(ii) and (iii), respectively. The generated OCS-UWB signal is amplified by an erbium-doped fiber amplifier (EDFA) and a tunable optical filter (TOF) is used to suppress amplified spontaneous emission (ASE) noise. After transmission over a 25-km standard single-mode fiber (SSMF), a high-speed PD is used to convert the OCS-UWB signal into an electrical UWB signal. Fig. 5(iv) and (v) provides the waveforms of one filtered sideband of the OCS-UWB signal. The frequency spacing of the two tones generated by the OCS modulation is 20 GHz, and the spectrum range of the UWB pulses is more than 10 GHz, resulting in partial frequency overlapping between the two tones. However, the 10-dB bandwidths of the monocycle and doublet pulse are less than 10 GHz. Therefore, the impact of the frequency overlapping on the up-converted UWB signal is insignificant. One can obtain a 24-GHz UWB signal matched with the FCC standard after PD detection, which is verified by the electrical spectra indicated in Fig. 6. The up-converted UWB signal has a central frequency of $\sim$24 GHz and a 10-dB bandwidth of $\sim$6 GHz (from $\sim$21 to $\sim$27 GHz). A residual 20-GHz RF component is observed due to the OCS modulation. However, the undesired RF signal is located outside the bandwidth of the up-converted UWB pulses between 21 and 27 GHz, which can be easily filtered before radio propagation. Since the center frequency and the bandwidth of the UWB pulses are dependent on the pulsewidth, one important consideration is whether the UWB pulses are broadened after transmission. We provide measurements of the FWHM versus transmission distance. For a given temporal pulsewidth and time decay constant, the doublet pulse has lower bandwidth than the monocycle pulse. Thus, the doublet pulse shows better tolerance to dispersion, as indicated in Fig. 7(a). We also measure the BERs (bit-error rates) of the generated UWB signals, as provided in Fig. 7(b); the doublet pulse shows lower power penalty after 25-km transmission in the up-converted UWB over fiber system.

IV. CONCLUSION

We have proposed and experimentally demonstrated a 24-GHz UWB over fiber system, where a single DPMZM is used to generate UWB mo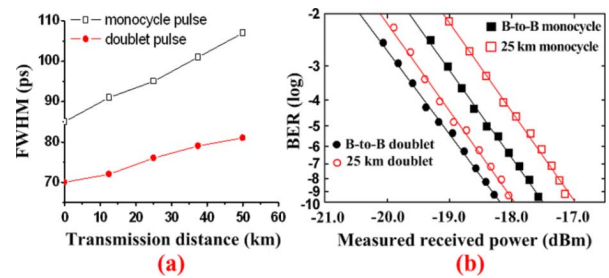nocycle or doublet pulses, and OCS modulation is employed to up-convert the UWB baseband to 24-GHz band. The proposed scheme may provide an effective solution for distribution of 24-GHz UWB over fiber systems.

REFERENCES

[1] D. Porcine, P. Research, and W. Hirt, "Ultra-wideband radio technology: Potential and challenges ahead," *IEEE Commun. Mag.*, vol. 41, no. 7, pp. 66–74, Jul. 2003.

[2] J. Yao, F. Zeng, and Q. Wang, "Photonic generation of ultrawideband signals," *J. Lightw. Technol.*, vol. 25, no. 11, pp. 3219–3235, Nov. 2007.

[3] J. Dong, X. Zhang, J. Xu, D. Huang, S. Fu, and P. Shum, "Ultrawideband monocycle generation using cross-phase modulation in a semiconductor optical amplifier," *Opt. Lett.*, vol. 32, no. 10, pp. 1223–1225, May 2007.

[4] Q. Wang, F. Zeng, S. Blais, and J. Yao, "Optical ultra-wideband monocycle pulse generation based on cross-gain modulation in a semiconductor optical amplifier," *Opt. Lett.*, vol. 31, no. 21, pp. 3083–3085, Nov. 2006.

[5] H. Chen, M. Chen, C. Qiu, and S. Xie, "A novel composite method for ultra-wideband doublet pulses generation," *IEEE Photon. Technol. Lett.*, vol. 19, no. 24, pp. 2021–2023, Dec. 15, 2007.

[6] F. Zeng and J. Yao, "Ultrawideband impulse radio signal generation using a high-speed electrooptic phase modulator and a fiber-Bragg-grating-based frequency discriminator," *IEEE Photon. Technol. Lett.*, vol. 18, no. 19, pp. 2062–2064, Oct. 1, 2006.

[7] F. Zeng, Q. Wang, and J. P. Yao, "All-optical UWB impulse generation based on cross phase modulation and frequency discrimination," *Electron. Lett.*, vol. 43, no. 2, pp. 119–121, Jan. 2007.

[8] V. T. Company, K. Prince, and I. T. Monroy, "Fiber transmission and generation of ultrawideband pulses by direct current modulation of semiconductor lasers and chirp-to-intensity conversion," *Opt. Lett.*, vol. 33, no. 3, pp. 222–224, Feb. 2008.

[9] C. Wang, F. Zeng, and J. Yao, "All-fiber ultra wideband pulse generation based on spectral shaping and dispersion-induced frequency-to-time conversion," *IEEE Photon. Technol. Lett.*, vol. 19, no. 3, pp. 137–139, Feb. 1, 2007.

[10] T. Kawanishi, T. Sakamoto, and M. Izutsu, "Ultra-wide-band radio signal generation using optical frequency-shift-keying technique," *IEEE Microw. Wireless Compon. Lett.*, vol. 15, no. 3, pp. 153–155, Mar. 2005.

[11] FCC, Second Report and Order and Second Memorandum Opinion and Order FCC 04-285 Dec. 2004.

[12] Y. L. Guennec and R. Gary, "Optical frequency conversion for millimeter-wave ultra-wideband-over-fiber systems," *IEEE Photon. Technol. Lett.*, vol. 19, no. 13, pp. 996–998, Jul. 1, 2007.

[13] T. Kuri, Y. Omiya, T. Kawanishi, S. Hara, and K. Kitayama, "Optical transmitter and receiver of 24-GHz ultra-wideband signal by direct photonic conversion techniques," in *Int. Topical Meeting Microwave Photonics*, Grenoble, France, Oct. 2006.

[14] K. Higuma, S. Oikawa, Y. Hashimoto, H. Nagata, and M. Izutsu, "X-cut lithium niobate optical single-sideband modulator," *Electron. Lett.*, vol. 37, no. 8, pp. 515–516, Apr. 2001.

[15] Q. Chang, H. Fu, and Y. Su, "Simultaneous generation and transmission multi-band signals and upstream data in a bidirectional radio over fiber system," *IEEE Photon. Technol. Lett.*, vol. 20, no. 3, pp. 181–183, Feb. 1, 2008.